1907 Static Liquefaction Flow Failure of the North Dike of Wachusett Dam

By Scott M. Olson,[1] Student Member, ASCE,
Timothy D. Stark,[2] William H. Walton,[3] Members, ASCE, and Gonzalo Castro,[4] Fellow, ASCE

Abstract: A static liquefaction flow failure occurred in the upstream slope of the North Dike of Wachusett Dam near Clinton, Massachusetts on April 11, 1907 during the first reservoir filling. The fine sands of the upstream dike shell liquefied and flowed approximately 100 m horizontally into the reservoir. This paper presents a description of the construction of the North Dike, failure of the upstream slope, and the results of stability analyses that were conducted to estimate the shear strength mobilized in the liquefied soils during failure. Analyses of the postfailure geometry, the prefailure geometry, and an analysis incorporating the kinetics of failure were conducted. The back-calculated shear strength considering the kinetics of failure is in agreement with other liquefaction flow failure case histories published in the literature. As a result, it is recommended that the kinetics of failure be considered to determine the shear strength mobilized during a liquefaction flow failure.

INTRODUCTION

The Wachusett Reservoir was conceived in the late 19th century to supply the metropolitan Boston region with potable water. The Wachusett Dam and Reservoir is situated on the South Branch of the Nashua River in Clinton, Massachusetts, located approximately 48 km west of Boston, as indicated in Fig. 1. The 246-billion liter reservoir was metro-Boston's largest water supply for 33 years until the construction of the 1.56-trillion liter Quabbin Reservoir in 1939. Today, the Wachusett Reservoir is still an integral element in the metro-Boston water supply and distribution system (Baril et al. 1992).

Construction of the main dam and supporting dikes began in 1898 and was completed in 1907. The main dam is a stone masonry, gravity structure, 43 m high and 259 m long with a crest elevation of 126.7 m (Boston City Datum; all elevations herein are based on this reference elevation, which is 1.72 m below mean sea level). The 3,200 m long North Dike and 760 m long South Dike were constructed in natural low lying areas along portions of the reservoir rim. The North Dike has approximate minimum and maximum crest elevations of 123.6 and 125.9 m, respectively, and traverses a relict glacial lake. The South Dike has a crest elevation of 123.7 m and is situated in a low area known as the Carville Basin (Baril et al. 1992). The North and South Dikes are zoned earth fill dams consisting of a sandy silt to silty sand central core and supporting shells comprised mainly of fine sand. The layout of the main dam and supporting dikes is shown in Fig. 1.

On April 11, 1907, during the first filling of the reservoir, a slope failure occurred in a portion of the upstream slope of the eastern section of the North Dike. The construction method, loading prior to failure (i.e., reservoir filling), and failure morphology suggest that liquefaction of the loose sandy fill within the upstream shell led to the observed slope failure. This failure is considered a "static liquefaction flow failure" because a loss of strength in the upstream soils occurred, leading to the observed flow slide. It is considered static because no seismic or dynamic forces were involved in the failure movements. Gravitational forces alone drove the failure movements. This is similar to the failure movements accompanying the static liquefaction flow failures of Calaveras Dam (Hazen 1918) and Fort Peck Dam (Casagrande 1965).

The present paper presents a description of the construction, failure, and reconstruction of the North Dike, as well as stability analyses of the failed portion of the upstream slope of the North Dike. The stability analyses include analyses of the postfailure geometry, prefailure geometry, and analyses that incorporate the kinetics, i.e., momentum, of failure to estimate the shear strength mobilized in the liquefied soils during flow. Incorporating kinetics led to a back-calculated shear strength significantly higher than the shear strength back-calculated from the postfailure geometry. Throughout this paper, the term "kinetics" is used rather than "dynamics" because kinetics describes the mechanics of movement, i.e., the forces and ac-

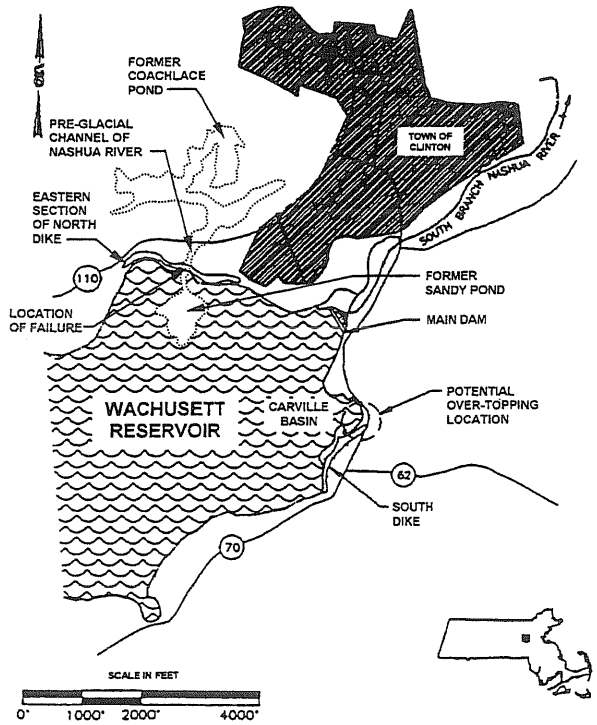

FIG. 1. Wachusett Water Supply Reservoir—Plan Locations of Main Dam, North Dike, South Dike, Former Coachlace and Sandy Ponds, Preglacial Channel of Nashua River, and Approximate Location (Station 23+20) of 1907 Slope Failure (after Baril et al. 1992)

[1]Grad. Res. Asst., Univ. of Illinois, Urbana-Champaign, Dept. of Civ. and Envir. Engrg., Urbana, IL 61801.
[2]Prof. of Civ. and Envir. Engrg., Univ. of Illinois, Urbana-Champaign, Dept. of Civ. and Envir. Engrg., Urbana, IL.
[3]Prin. Engr., STS Consultants, Ltd., Vernon Hills, IL 60061-3153.
[4]Prin., GEI Consultants, Inc., Winchester, MA 01890-1970.

Note. Discussion open until May 1, 2001. To extend the closing date one month, a written request must be filed with the ASCE Manager of Journals. The manuscript for this paper was submitted for review and possible publication on August 10, 1999. This paper is part of the *Journal of Geotechnical and Geoenvironmental Engineering*, Vol. 126, No. 12, December, 2000. ©ASCE, ISSN 1090-0241/00/0012-1184–1193/$8.00 + $.50 per page. Paper No. 21610.

celerations acting on the failure mass. The term dynamics is typically associated with inertia forces imposed by earthquake shaking, and is not used to avoid confusion.

LOCAL SOIL CONDITIONS AND SITE GEOLOGY

The following descriptions of the site conditions and dike construction, failure, and reconstruction are summarized from GZA GeoEnvironmental, Inc. (1991); an unpublished report by D. D. Ashenden, Massachusetts Water Resource Authority (1991); Haley & Aldrich, Inc. (1984a,b); and Metropolitan District Commission (1907). These sources utilized English units, and thus English units with metric equivalents are used in some of the figures.

The eastern section of the North Dike of Wachusett Dam is located in a preglacial valley of the Nashua River. Following glaciation, the Nashua River rerouted to its present course, and this valley became a sand and gravel plain. The eastern section of the North Dike crosses a former river channel that connected the Coachlace Pond to the north and Sandy Pond to the south prior to impoundment (Fig. 1). Fig. 2 presents a longitudinal cross section of the eastern section of the North Dike along the centerline of the main cut-off wall and core. As indicated in Fig. 2, the cut-off wall and core extend over the entire length of the North Dike, and the dike has a maximum height of 24.4 m over the river channel. The natural soils underlying the North Dike generally consist of dense to very dense sands, gravels, and nonplastic silts. Along the former river channel, an intermittent natural organic silt and fibrous peat deposit is present.

Prior to construction of Wachusett Dam and the supporting dikes, over 1,000 borings were drilled along the proposed location of the North Dike. One boring located 61 m west of the channel south from Coachlace Pond encountered bedrock at approximately 91 m below the ground surface. No other boring reached bedrock, but based on local geology, bedrock is estimated to be on the order of 150 m below the original ground surface.

CONSTRUCTION, FAILURE, AND RECONSTRUCTION OF NORTH DIKE

The 3,200 m long North Dike was constructed using controlled placement and compaction for the cut-off wall and core materials and uncontrolled fill methods for the shells. Construction of the North Dike began in 1898 with the excavation of main and secondary cut-off trenches. Trench excavation was completed in 1899. Backfilling of the trenches commenced in 1900 and was completed in 1901.

In 1902, construction of the dike sections began. The materials for the core were stripped from the reservoir area and consisted of sandy silt to silty sand. A large portion of the shell fill soils consisted of fine sand, which was spoil from the cut-off trenches. The core soils were placed in 0.15 m lifts and rolled by horse-drawn carts. No direct measurements of the density of the core material were made, either at the time of construction or duing the recent investigations. However, tube samples obtained during the recent investigations indicated saturated unit weights in the range of 18.9 to 20.4 kN/m^3. The core was sloped in the upstream direction of the dam at a slope of 1 horizontal to 1 vertical (1H:1V) and has a maximum width of approximately 30.5 m. The prefailure cross section of the North Dike near the location of the slope failure (centered near Station 23+20) is presented in Fig. 3.

The downstream shell fill consists of sand to silty sand with some gravel. The downstream shell soils reportedly were placed in 2.3 m lifts and were compacted by flooding with water. Approximately 0.15–0.3 m of settlement was observed following saturation of each 2.3 m lift. The slope of the downstream shell varies from 4H:1V immediately downstream of

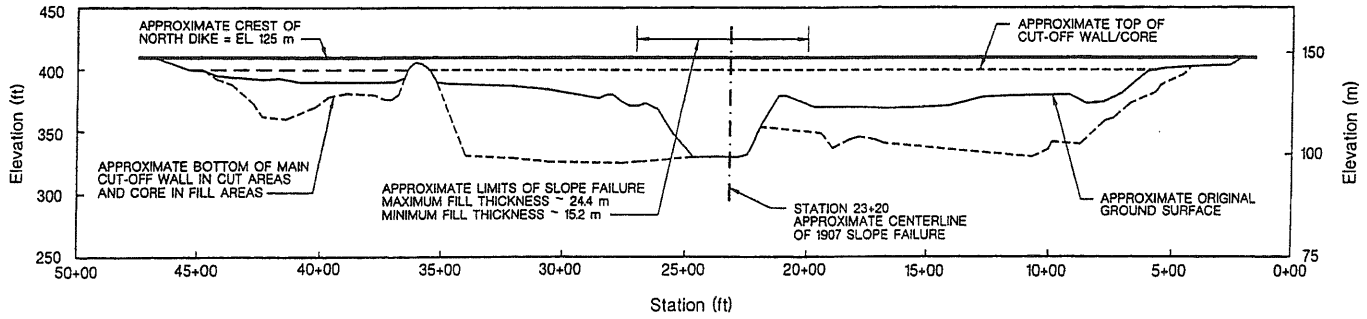

FIG. 2. Longitudinal Cross Section of the North Dike of Wachusett Dam along the Centerline of the Main Cut-Off Wall and Core Showing the Locations of the Stream Channel and 1907 Slope Failure (5x Vertical Exaggeration)

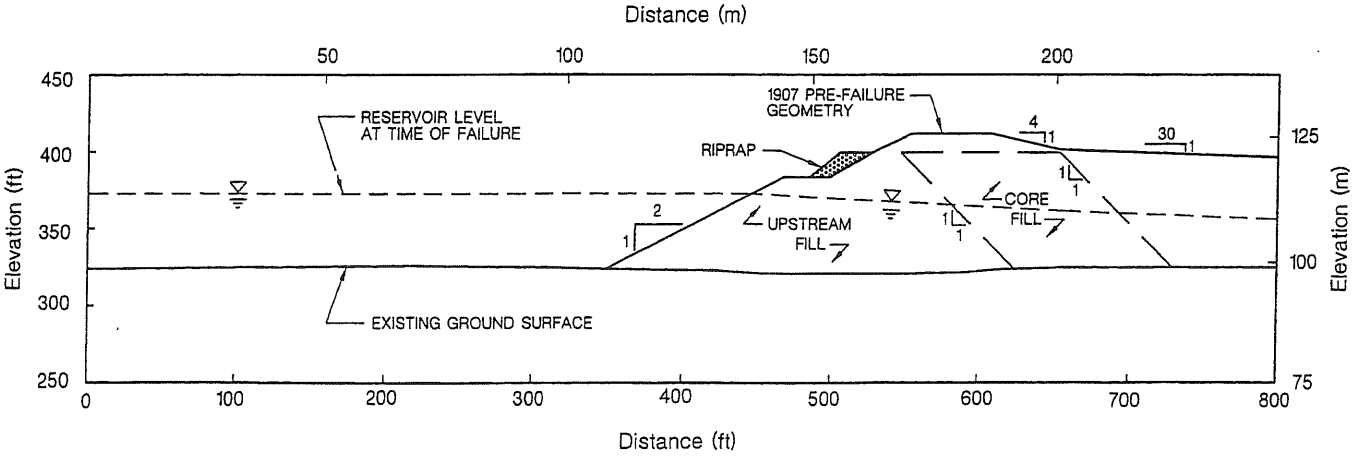

FIG. 3. Prefailure Cross Section of the North Dike of Wachusett Dam at Station 23+20

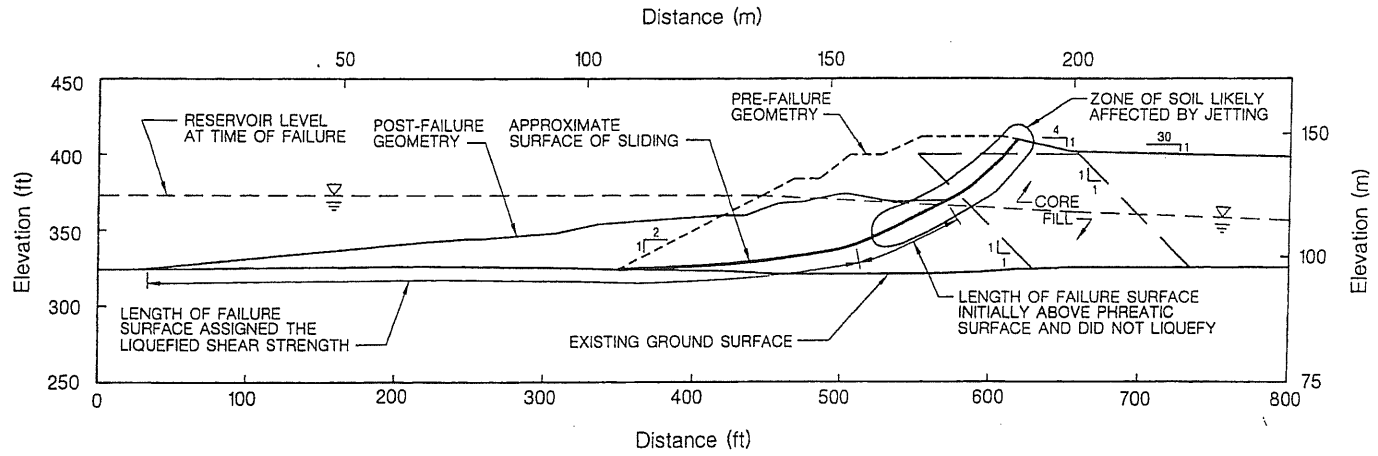

FIG. 4. Cross Section through the Failed Portion of the North Dike of Wachusett Dam Showing the Approximate Location of the Sliding Surface through the Dike

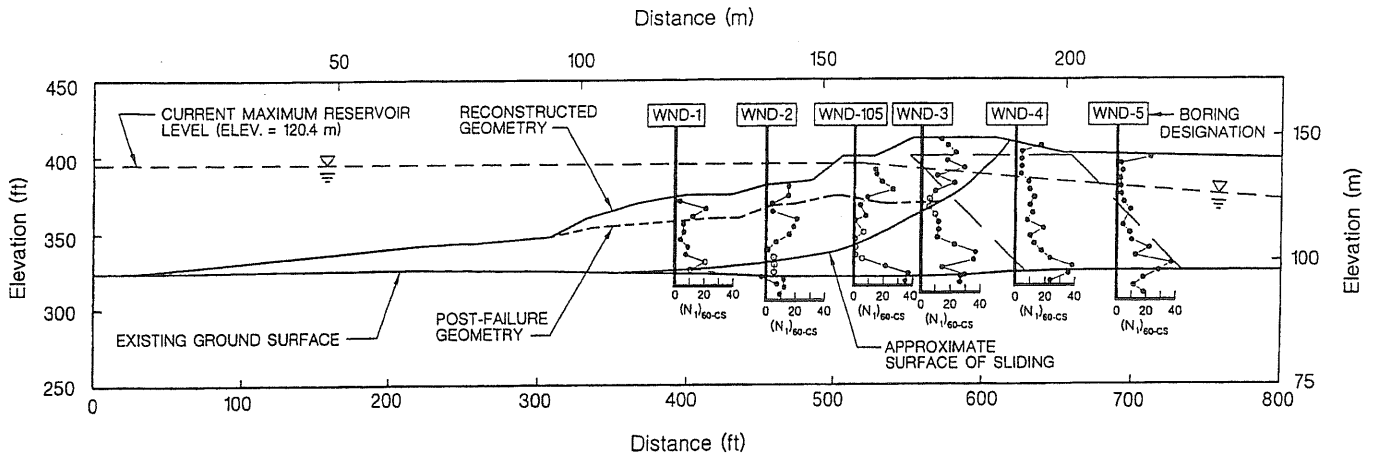

FIG. 5. Reconstructed Cross Section of the North Dike of Wachusett Dam at Station 23+20 Showing the Locations and Results of Recent Standard Penetration Tests

the crest to approximately elevation 122.5 m, then slopes at 30H:1V toward Coachlace Pond, as indicated in Fig. 3.

The upstream shell fill also consists of sand to silty sand with some gravel. Unlike the downstream fill, the upstream fill received no compaction or saturation. The upstream fill was placed at a 2H:1V to 3H:1V slope from the crest of the dike to a 6 m wide bench at approximately elevation 122.5 m. The bench consists of riprap placed at a slope of 1.25H:1V to approximately elevation 117 m. Below this elevation, the shell was placed at a slope of 2H:1V from the existing ground surface, as shown in Fig. 3.

Fill placement for the North Dike was completed in 1904, three years prior to the slope failure. In-situ permeability tests conducted during recent investigations indicated that the upstream and downstream shell soils have a permeability on the order of 1×10^{-5} m/s. Therefore, based on the elapsed time and the high permeability of the shell soils, it is highly unlikely that any excess porewater pressures resulting from saturation existed in the fill at the time of the slope failure.

On April 11, 1907, a slope failure occurred during initial filling of the reservoir. The failure involved approximately 46,500 m^3 of material from a 213 m long section of the North Dike. The failure was centered over the former river channel (between Stations 22+50 and 25+00), where the dike reached its maximum height of 24.4 m. The reservoir was approximately at elevation 114 m, or a depth of 12.8 m, at the time of failure. As indicated in Fig. 4, the failure mass flowed into the reservoir for a maximum horizontal distance of approximately 100 m and the crest dropped a maximum vertical distance of approximately 12 m. The failure mass came to rest below the reservoir water level at an angle of approximately 5 to 6 degrees.

The failed zone of the North Dike was rebuilt in 1907 at a slope approximately 4H:1V to 5H:1V (prior to failure the upstream slope was 2H:1V) by dumping fill soils into the reservoir to form a 9 to 17 m wide berm to approximately 0.6 m above the postfailure reservoir level. No attempt was made to remove the slide mass, and dumped fill was placed atop the slide mass without compaction. Loose or cracked portions of the embankment above the berm level were excavated, and the original dike geometry of approximately 2H:1V was maintained by placing granular fill in 0.3 m lifts, compacting it with horse-drawn carts, and saturating the fill with water pumped from the reservoir. Above the berm level, jets of water were forced into the fill along the interface between the new and old construction to promote mixing and cosedimentation of the materials. Reconstruction was completed on October 30, 1907, and reservoir filling was resumed without incident to a maximum pool elevation of approximately 120 m. An approximate cross section of the North Dike at Station 23+20 following reconstruction is presented in Fig. 5.

Density of Upstream Shell Soils

As a part of a GZA GeoEnvironmental, Inc. (1991) geotechnical study, numerous borings and standard penetration tests (SPTs), as well as a suite of laboratory tests, were conducted. The purpose of the GZA study was to investigate the

current seismic stability of the North Dike. Borings drilled in 1983 within the zone of the 1907 slope failure as part of a Haley & Aldrich, Inc. (1984a,b) geotechnical study are also available. Values of corrected SPT blowcount (Seed et al. 1985) were calculated as

$$(N_1)_{60} = N \frac{ER}{60} C_N \quad (1)$$

where N = field SPT blowcount; ER = energy ratio of the SPT system used in the field; and C_N = overburden correction (Liao and Whitman 1986), expressed as

$$C_N = 1/(\sigma'_v)^{0.5} \quad (2)$$

where σ'_v = vertical effective stress in tons per square foot (100 kPa). All borings were drilled using mud rotary techniques, and SPT tests were conducted using a "donut ring" hammer. Therefore, an energy ratio (ER) of 45% was applied (Seed et al. 1985).

As indicated in Fig. 5, six borings were drilled in the 1980's and 1990's in the reconstructed portion of the North Dike along Station 23+20. Based on the soil descriptions from the boring logs, it appears that thirty SPT tests were conducted in the shell soils involved in the 1907 failure. The $(N_1)_{60}$ values in these soils average 8 blows per foot (bpf; blows/0.3 m), with a range of 1–21 bpf. Thirteen SPT tests were conducted near the estimated failure surface of the 1907 flow failure. These $(N_1)_{60}$ values are shown as open circles in Fig. 5 and average around 6 to 7 bpf. Therefore, an $(N_1)_{60}$ value of 7 bpf was considered representative of the density of the upstream shell soils (as measured between 1983 and 1991) that liquefied during the 1907 failure. This value is in agreement with other $(N_1)_{60}$ values measured during the recent investigations in both the upstream and downstream shell of the North Dike outside of the 1907 failure zone.

Reconstruction of the North Dike involved the placement of up to 6.1 m (with an average thickness of approximately 4.6 m) of new fill over the shell material that had liquefied and failed. The liquefied soils probably reconsolidated under their own weight by the time the new fill was placed and further consolidated due to the weight of the added fill. Thus it is possible that the prefailure density of the soils that liquefied was lower than that indicated by the blowcounts recently measured in the reconstructed dike. In addition, granular soils are known to exhibit an increase in penetration resistance following disturbance or densification as a result of secondary compression and aging (Schmertmann 1987; Mesri et al. 1990). As there is no rational means to estimate the density changes and aging effects from 1907 to 1991, it was concluded that the current average $(N_1)_{60}$ value of 7 bpf may be higher than the actual value of $(N_1)_{60}$ at the time of failure in 1907. The jetting of water that was done as a part of reconstruction likely only affected fill soils near to and above the phreatic surface in the North Dike, as illustrated in Fig. 4. Therefore, it is unlikely that the jetting of water significantly affected the measured $(N_1)_{60}$ values, with the possible exception of those measured in boring WND-3.

The soil in the estimated failure zone has a representative median grain size, D_{50}, of approximately 0.42 mm and a fines content of 5–10%. As aforementioned, the permeability of the shell soils was measured to be approximately 1×10^{-5} m/s. As a result, it is reasonable to assume that the phreatic surface in the upstream shell reached hydraulic equilibrium almost immediately during the first filling of the reservoir. The core consists of sandy silt to silty sand and has a lower permeability than the shell soils. Therefore, a change in the slope of the phreatic surface at the core (compared to the slope of the phreatic surface in the upstream shell) would occur during first filling of the reservoir. However, the position of the phreatic surface in the core has no effect on the stability calculations presented herein. As shown in Figure 4, the failure surface crosses the core material above the phreatic surface and reservoir level at the time of failure. Therefore, the slope of the phreatic surface through the North Dike at the time of failure was assumed to be parallel to the steady-state slope of the phreatic surface measured as a part of the GZA GeoEnvironmental, Inc. (1991) study.

STABILITY ANALYSES OF NORTH DIKE SLOPE FAILURE

The stability analyses for the liquefaction flow failure of the North Dike described herein were conducted using the cross section at Station 23 + 20. These analyses included:

- Back-calculation of a lower-bound shear strength and shear strength ratio from the postfailure geometry.
- Back-calculation of an upper-bound shear strength and shear strength ratio from the prefailure geometry.
- Back-calculation of the liquefied shear strength and liquefied shear strength ratio considering the kinetics (i.e., momentum) of failure.

Based on a recent National Science Foundation Workshop (Stark et al. 1998), a general term, liquefied shear strength, is used to describe the shear strength mobilized during a liquefaction flow failure. Other terms have been used to describe this shear strength, e.g., undrained residual shear strength (Seed 1987), undrained steady-state shear strength (Poulos et al. 1985), and undrained critical shear strength (Stark and Mesri 1992). The liquefied shear strength ratio is defined as the liquefied shear strength divided by the prefailure vertical effective stress in the zone of liquefaction. The concept of a liquefied strength ratio was proposed by Stark and Mesri (1992), and was termed the undrained critical strength ratio.

The possibility that three-dimensional effects influenced the shear strength mobilized during the failure of the North Dike was considered using the procedures developed by Stark and Eid (1998) and Skempton (1985). The failure of the North Dike was approximately 213 m in width (Fig. 2) and the depth of the failure surface averaged approximately 9 m (Fig. 4). For these failure dimensions, both methods indicate that the potential three-dimensional effect was negligible, and therefore was not used in the following analyses.

Postfailure Geometry Analyses

Seed (1987) conducted limit-equilibrium stability analyses of the postfailure slope geometry (for most of the cases) to back-calculate the liquefied shear strength mobilized during a number of liquefaction flow failures and lateral spreads. For a given case, the value of shear strength in the assumed liquefied soil was varied until a factor of safety of unity was achieved in the stability analysis. However, Davis et al. (1988) illustrated the importance of kinetics, or momentum, on the back-calculated shear strength. The effect of kinetics during a flow failure can result in the shear strength back-calculated from the postfailure geometry being considerably lower than the value of shear strength actually mobilized during the failure. Therefore, the postfailure geometry analyses were considered to provide lower-bound estimates of the liquefied shear strength and strength ratio.

Examining the prefailure and postfailure geometry, a reasonable failure surface for the North Dike was ascertained, as shown in Fig. 4. The failure surface was divided into a liquefied and nonliquefied zone. The nonliquefied zone accounts for the fill soils that initially were above the phreatic surface and did not liquefy. These soils were assumed to be drained

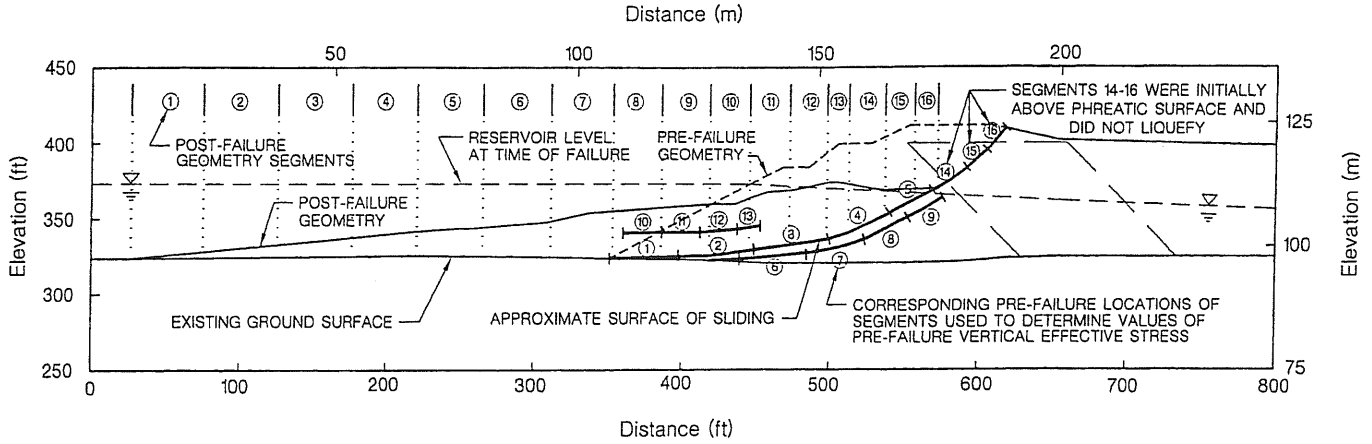

FIG. 6. Determination of Prefailure Vertical Effective Stresses for Liquefied Shear Strength Ratio Analysis

during failure and were assigned an effective constant volume (or steady-state) friction angle ϕ'_{cv}, of 30°. In the first analysis, the shear strength in the liquefied zone was varied until a factor of safety of unity was achieved, as suggested by Seed (1987). The slope stability analyses were conducted using Spencer's (1967) stability method as coded in the microcomputer program UTEXAS3 (Wright 1990).

A second analysis was conducted using the same postfailure slope geometry to obtain a lower-bound value of liquefied strength ratio. This was accomplished by assuming that the initial failure surface passes approximately through the center of the zone of liquefaction. Thus, the actual extents of the zone of liquefaction did not need to be determined. The postfailure sliding surface was divided into 16 segments, as shown in the upper portion of Fig. 6. Segments 1–13 correspond to liquefied soils (identical to the length of liquefied soil in Fig. 4), while segments 14–16 correspond to soils initially above the phreatic surface that did not liquefy. Based on the lengths of the postfailure segments, corresponding lengths of liquefiable soil were defined within the prefailure geometry. Segments 1–5 were located on the initial failure surface, while segments 6–9 and segments 10–13 were placed equal distances below and above the initial failure surface, respectively. Additional analyses showed that rearranging the positions of the segments had little effect on the back-calculated liquefied strength ratio, as long as the segments were centered around the initial failure surface.

Prefailure vertical effective stresses (σ'_{vo}) were determined for segments 1–13 (i.e., the liquefied soil) in their prefailure positions and were assigned to the corresponding segments in their postfailure positions. Using the individual σ'_{vo} values for each segment and a single value of liquefied strength ratio, individual values of liquefied shear strength were assigned to each postfailure geometry segment for the stability analysis. This allows the liquefied shear strength to model the variation in pre-failure σ'_{vo} of the liquefied soil along the final sliding surface. Segments 14–16 were initially above the phreatic surface and were assigned a ϕ'_{cv} = 30°. The liquefied strength ratio was then varied (which in turn varies the liquefied shear strength mobilized along segments 1–13) until a factor of safety of unity was achieved.

The analyses of the postfailure geometry yielded the following results:

- Lower bound liquefied shear strength ≅ 3.8 kPa
- Lower bound liquefied shear strength ratio ≅ 0.026

A weighted average prefailure vertical effective stress of 151.2 kPa was calculated for segments 1–13 (segments 14–16 did not liquefy) as follows

$$\sigma'_{v,\text{ave}} = \frac{\sum_{i=1}^{n} \sigma'_{v,i} L_i}{L_{\text{total}}} \tag{3}$$

where $\sigma'_{v,\text{ave}}$ = weighted average vertical effective stress; $\sigma'_{v,i}$ = vertical effective stress of the ith segment of the failure mass; L_i = length of the ith segment of the failure surface; and L_{total} = total length of the liquefied portion of the failure surface.

Multiplying the liquefied shear strength ratio of 0.026 by the weighted average prefailure vertical effective stress of 151.2 kPa yields a shear strength of 3.9 kPa. This value agrees with the liquefied shear strength of 3.8 kPa back-calculated independently. This agreement suggests that the liquefied strength ratio analysis provides an appropriate lower bound strength ratio.

Prefailure Geometry Analyses

The mechanism triggering liquefaction in the upstream shell of the North Dike was likely a decrease in effective stress due to reservoir filling under a nearly shear stress. The failure occurred at the location where the driving shear stress was largest (i.e., at the location of the maximum dike height). As the reservoir level rose, the vertical effective stress within the upstream shell decreased considerably. However, as about half of the dike was still above the phreatic surface at the time of the failure, the shear stress on the failure surface only decreases slightly (about 15%). Sasitharan et al. (1993) showed that this stress path triggers liquefaction in loose sands if the stress conditions reach the collapse surface (as defined by Sladen et al. 1985) and the driving shear stress is greater than the liquefied shear strength. At the moment of failure, i.e., when the factor of safety against slope failure is equal to unity, the shear strength mobilized just prior to collapse and liquefaction should be representative of the peak undrained shear strength. This shear strength also represents an upper bound of the liquefied shear strength because the liquefied shear strength must be less than this value for a flow failure to occur. Therefore, a back-analysis of the prefailure geometry determines an upper bound to the liquefied shear strength. Using the prefailure geometry and the failure surface shown in Fig. 4, values of shear strength below the phreatic surface were varied until a factor of safety of unity was achieved. Soils above the phreatic surface were assigned ϕ' = 30° to 35°.

A second analysis using the same prefailure slope geometry was conducted to obtain an upper bound strength ratio mobilized at the onset of failure. This was accomplished by assuming that the indicated failure surface passes approximately through the center of the zone of liquefaction. Thus, the actual

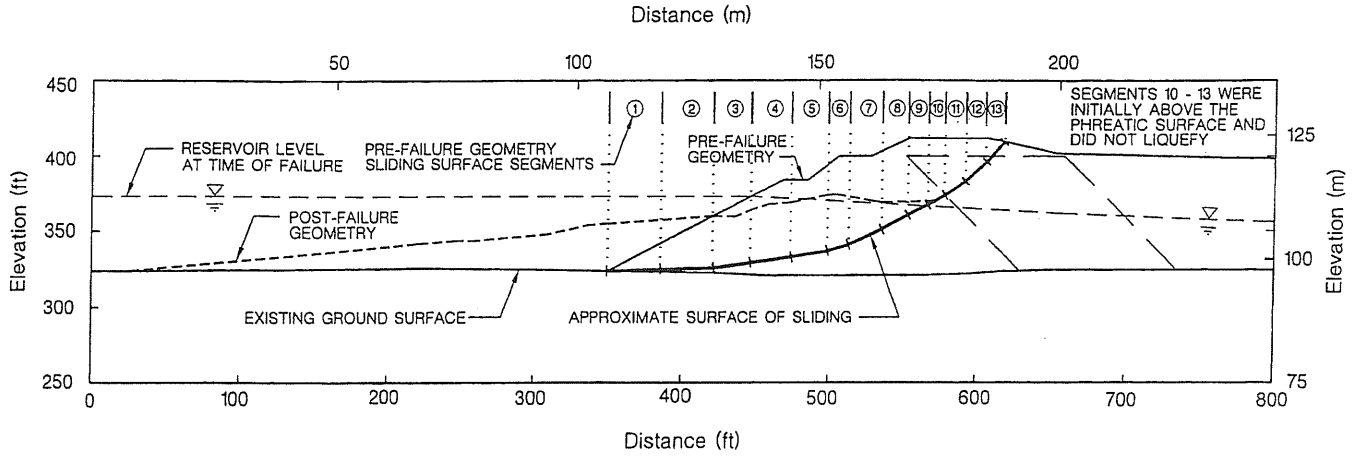

FIG. 7. Determination of Prefailure Vertical Effective Stresses for Upper Bound Shear Strength Ratio Analysis

zone of liquefaction did not need to be estimated. The initial sliding surface was divided into 13 segments, as shown in Fig. 7. Segments 1–9 correspond to liquefied soils (i.e., loose shell soils below the phreatic surface), while segments 10–13 correspond to soils above the phreatic surface that did not liquefy. Prefailure vertical effective stresses (σ'_{vo}) were determined for segments 1–9 in Fig. 7 (i.e., the liquefied soil). Using the individual σ'_{vo} values for each segment and a single value of strength ratio, individual values of shear strength were assigned to each segment for the stability analysis. The strength ratio was then varied (which in turn varies the shear strength mobilized along segments 1–13 until a factor of safety of unity was achieved.

The analyses of the prefailure geometry yielded the following results:

- Upper bound shear strength $\cong$ 37.6 to 41.9 kPa
- Upper bound strength ratio $\cong$ 0.26 to 0.30

The upper values of the ranges correspond to $\phi' = 30°$ in the nonliquefied soils (segments 10–13 in Fig. 7) and the lower values of the ranges correspond to $\phi = 35°$ in the nonliquefied soils.

A weighted average prefailure vertical effective stress of 141.6 kPa can be calculated for segments 1–9 (in Fig. 7) using (3). Multiplying the upper bound strength ratio of 0.26–0.30 by the $\sigma'_{v,ave}$ of 141.6 kPa yields a shear strength of 36.8–42.6 kPa. This range agrees with the upper bound shear strength of 37.6–41.9 kPa back-calculated independently. This agreement suggests that the upper bound strength ratio analysis provides an appropriate value of strength ratio.

It should be noted that the weighted average vertical effective stress of 141.6 kPa for the upper-bound strength ratio analysis differs slightly from the weighted average vertical effective stress of 151.2 kPa for the lower bound strength ratio analysis. The reason for this difference is probably related to the volume of soil involved in the failure. The initial failure of the North Dike probably involved a relatively well-defined failure zone, while during failure, more soil liquefied and became involved in the failure and failure zone.

Analysis Considering Kinetics of Failure Mass Movements

To obtain a best estimate of liquefied shear strength mobilized during failure, the stability analysis should consider the kinetics of failure. The reason for this is illustrated in Fig. 8. At the onset of a liquefaction flow failure, only small strains are required to reduce the shear strength from the peak to the liquefied value (Davis et al. 1988). These strains occur while

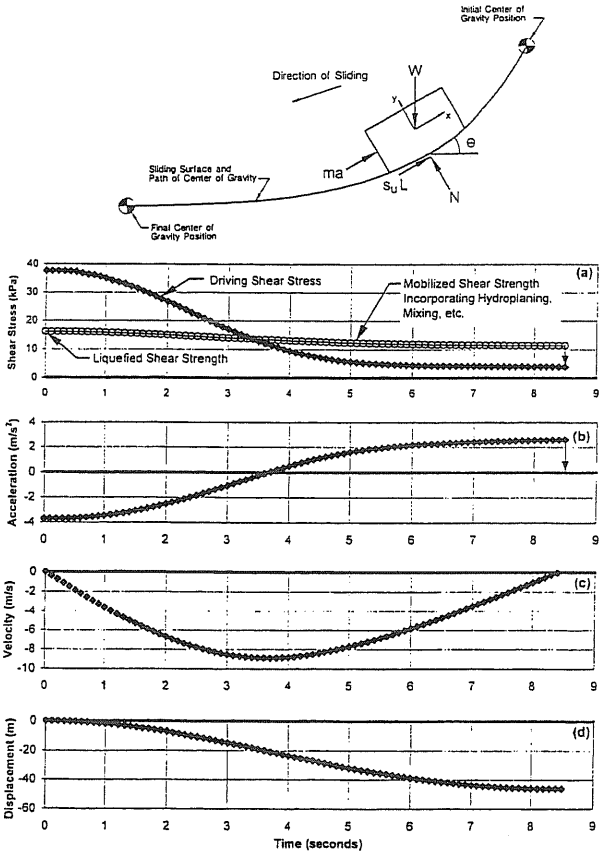

FIG. 8. Example Freebody Diagram Used for Kinetics Analysis and Kinetics Analysis Results for North Dike of Wachusett Dam

the driving shear stress remains relatively unchanged. Therefore, for simplification, this analysis assumes that the liquefiable soil is in a postpeak condition at the beginning of failure (at time, $t = 0$), and thus the mobilized strength is equal to the liquefied shear strength, as indicated in Fig. 8(a). The average initial driving shear stress was estimated in the prefailure geometry analysis as 37.6 kPa. Because the driving shear stress is larger than the liquefied shear strength (this is a prerequisite for a liquefaction flow failure), the mass begins to accelerate downslope [Fig. 8(b)]. Therefore, the velocity of the failure mass increases from zero [Fig. 8(c)], and downslope displacement occurs [Fig. 8(d)]. The downslope displacement of the failure mass, in turn, decreases the driving shear stress of the failure mass because of the curvature of the failure path.

When the driving shear stress is reduced to a value equal

to the mobilized shear strength, the failure mass has an acceleration of zero and has attained its maximum velocity [Figs. 8(b) and 8(c)]. In Fig. 8(a), the mobilized shear strength decreases from the liquefied shear strength as a result of hydroplaning, as discussed subsequently. Because the failure mass has a finite velocity, it continues to displace and deform, decreasing the driving stress to a value less than the mobilized shear strength, thereby decelerating the failure mass [i.e., upslope acceleration; Figs. 8(a) and 8(b)]. When the failure mass reaches a velocity of zero and comes to rest, the driving shear stress may be considerably less than the liquefied shear strength [Fig. 8(a)]. At the instant the failure mass comes to rest, the mobilized shear strength is assumed to decrease to that required for static stability, i.e., the driving shear stress of the postfailure geometry [Fig. 8(a)].

The kinetics analysis conducted for this study was adapted from the procedure outlined by Davis et al. (1988) and is reviewed briefly. The analysis is based on Newton's second law of motion, as follows (in vector form):

$$\mathbf{F} = m \cdot \mathbf{a} \tag{4}$$

where $\mathbf{F}$ = resultant (net) external force vector acting on the failure mass; m = mass of the failed material (weight divided by acceleration due to gravity, g); and $\mathbf{a}$ = acceleration vector of the center of gravity of the failed material in units of g. Referring to Fig. 8, the net external force, $\mathbf{F}$, acting on the failure mass in the direction of movement of the center of gravity is given by the driving weight of the failure mass minus the mobilized shear resistance of the soil, as follows:

$$\mathbf{F} = [(W \cdot \sin\theta) - (s_u \cdot L)] = m \cdot \mathbf{a} \tag{5}$$

where W = weight of the failure mass; θ = angle between the horizontal and the tangent of the curve describing the movement of the sliding mass center of gravity at any time; s_u = mobilized shear strength; and L = length of the failure surface. At the start of sliding, the weight term is larger than the shear strength term, and the resultant acceleration is downslope. Near the end of sliding, the weight term is smaller than the shear strength term, and the resultant acceleration is upslope (decelerating the failure mass).

The movement of the center of gravity of the failure mass of the North Dike was described using a third-order polynomial. Davis et al. (1988) used a hyperbolic function to describe the movement of the center of gravity, but it was found during this study that a third-order polynomial provided slightly better representation of the failure surface shown in Fig. 4. This is important because the center of gravity of the failure mass was assumed to move parallel to the failure surface. A third-order polynomial has the form:

$$y = ax^3 + bx^2 + cx + d \tag{6}$$

where a, b, c, and d = constants that are based on the x- and y-coordinates of the initial and final positions of the center of gravity of the failure mass and a curvature parallel to the failure surface. The values of these constants depend on the coordinate system used to define the geometry of the dike. Using the slope (dy/dx) of the curve described in (6) at any point, the sine of the angle θ is given by

$$\sin\theta = \frac{dy/dx}{\sqrt{1 + (dy/dx)^2}} \tag{7}$$

where dy and dx = vertical and horizontal displacements of the center of gravity of the failure mass along the curve defined by (6).

The acceleration of the center of gravity of the failure mass can be estimated using the second derivative of the displacement, Δ, with respect to time, t, as

$$\mathbf{a} = \frac{d^2\Delta}{dt^2} \tag{8}$$

Substituting into (4) yields the following equation:

$$[(W \cdot \sin\theta) - (s_u L)] = \frac{W}{g}\frac{d^2\Delta}{dt^2} \tag{9}$$

Eq. (9) can be solved numerically or by direct integration. For the analysis of the North Dike, a time-step numerical solution was obtained using a spreadsheet program. An initial value of liquefied shear strength was assumed and (9) was solved to estimate the total displacement and duration of movement. The assumed liquefied shear strength was then revised to achieve agreement between the computed and observed displacement of the center of gravity of the failure mass. No observation of the duration of failure was available, therefore no comparison was available for the computed duration of failure.

The kinetics analysis also should account for potential hydroplaning (slide material "riding" on a layer of water), mixing with water, and an increase in void ratio of the liquefied material as the failure mass slid into the reservoir (Castro et al. 1989; Castro 1995). To account for these potential effects, the shear strength mobilized along the failure surface in the reservoir (beyond the limits of the prefailure geometry) was assumed to be equal to 50% of the shear strength mobilized within the prefailure geometry limits of the dike. Reduction factors of 25% and 100% also were used to ascertain the sensitivity of the liquefied shear strength to the effect of hydroplaning and to obtain a range of possible values of liquefied shear strength. The same reduction factors were used by Castro et al. (1992) to back-calculate the possible range of liquefied shear strength mobilized during the flow failure of Lower San Fernando Dam.

The kinetics analysis also considered the change in weight of the failure mass as it slid into the reservoir, and the change in the length of the failure surface as the liquefied material flowed away from the core of the dike. These changes during failure were incorporated into the solution of (9) as a function of the distance traveled by the center of gravity of the failure mass with respect to its total distance of travel.

Results of Kinetics Analysis of North Dike of Wachusett Dam

The initial result of the kinetics analysis assumed that all soils along the failure surface mobilized the liquefied shear strength. This overestimated the actual liquefied shear strength because a portion of the failed soils initially were above the phreatic surface and did not liquefy, as aforementioned. Therefore, the liquefied shear strength was adjusted to account for the strength of the nonliquefied soils. Approximately 12% of the postfailure sliding surface length involved soils that did not liquefy. These soils (i.e., segments 14–16 in Fig. 6) were assigned an average shear strength of 47.8–57.4 kPa for values of ϕ of 30°–35°, respectively, and the liquefied shear strength was adjusted as follows:

$$s_u(\text{LIQ}) = \frac{s_u - \left(\frac{L_d}{100}\, s_d\right)}{\left(1 - \frac{L_d}{100}\right)} \tag{10}$$

where s_u was determined by the solution of (9), L_d = percentage of the total length of the postfailure sliding surface that incorporates soils that did not liquefy (approximately 12%); and s_d = average shear strength of the fill soils that did not liquefy (approximately 47.8–57.4 kPa).

TABLE 1. Summary of Stability Analyses of 1907 Slope Failure of North Dike of Wachusett Dam

Analysis (1)	Shear strength (kPa) (2)	Shear strength ratio (3)	Comments (4)
Postfailure geometry analysis	3.8	0.026	Lower bound shear strength and strength ratio back-calculated from postfailure geometry.
Prefailure geometry analysis	37.6–41.9	0.26–0.30	Upper bound shear strength and strength ratio back-calculated from prefailure geometry.
Analysis considering kinetics of failure mass movement	16.0 (10.4–19.1)	0.106 (0.070–0.126)	Best estimate of liquefied shear strength back-calculated considering kinetics of failure, hydroplaning, and shear strength of nonliquefied soils.

The kinetics analysis yielded the following results:

- Liquefied shear strength ≅ 16.0 kPa (range of 10.4–19.1 kPa)
- Liquefied shear strength ratio ≅ 0.106 (range of 0.070–0.126)

This liquefied shear strength resulted in a calculated displacement of the center of gravity of the failure mass of 9.4 m vertically and 44.5 m horizontally. This agrees well with the observed/measured center of gravity displacement of approximately 9.4 vertically and 44.8 m horizontally.

The kinetics analysis only provides a value of liquefied shear strength. Therefore, the liquefied shear strength ratio reported above was determined by dividing the liquefied shear strength of 16.0 kPa by the weighted average vertical effective stress of 151.2 kPa obtained from the postfailure geometry analysis.

These values of liquefied shear strength and strength ratio include the effects of kinetics, hydroplaning, and the shear strength of the soils that did not liquefy and therefore are considered best estimates. These values are roughly one-half of the sum of the upper and lower bounds computed from the prefailure and postfailure geometries, respectively. This result is reasonable because as illustrated in Fig. 8, the driving shear stress is approximately equal to the liquefied shear strength when the failed mass has moved about half-way between its prefailure and postfailure position. A summary of the results of all of the stability analyses is presented in Table 1.

COMPARISON WITH PUBLISHED VALUES FOR OTHER CASE HISTORIES

The best estimate values (and range of values) of liquefied shear strength and strength ratio obtained using the kinetics analysis (Table 1) are plotted with values obtained from case histories analyzed by Seed and Harder (1990) and Stark and Mesri (1992) in Figs. 9 and 10, respectively. The Seed and Harder (1990) data [which were used by Stark and Mesri (1992)] reportedly incorporate the kinetics of failure. However, Seed and Harder (1990) did not present their methodology to consider kinetics, and it may be different than the methodology used herein.

The Wachusett data point plots near the middle of the existing case histories in both figures. The Wachusett data point has an average $(N_1)_{60}$ of 7 bpf as explained earlier. However, the relationships of Seed and Harder (1990) and Stark and Mesri (1992) require that the value of $(N_1)_{60}$ be corrected for the presence of fines. The fines content of the shell soils of the North Dike is on the order of 5–10%. This results in a fines content correction, $\Delta(N_1)_{60}$, of 1 bpf, and an equivalent clean sand SPT blowcount, $(N_1)_{60\text{-}cs}$ of approximately 8 bpf for the Seed and Harder (1990) procedure. The Stark and Mesri (1992) procedure indicates that $\Delta(N_1)_{60}$ is 2.5 bpf, resulting in an $(N_1)_{60\text{-}cs}$ of 9.5 bpf. Therefore, the Wachusett data point is plotted with average $(N_1)_{60\text{-}cs}$ values of 8 and 9.5 bpf in Figs. 9 and 10, respectively. Additional uncertainty regarding the penetration resistance for this case is indicated by a dashed line and question mark to the left of the data point. The dashed lines and question marks in Figs. 9 and 10 signify that the blowcount value for the Wachusett data point (measured in the 1980's and 1990's) may be larger than the actual blowcount of the liquefied soils at the time of failure, as discussed earlier.

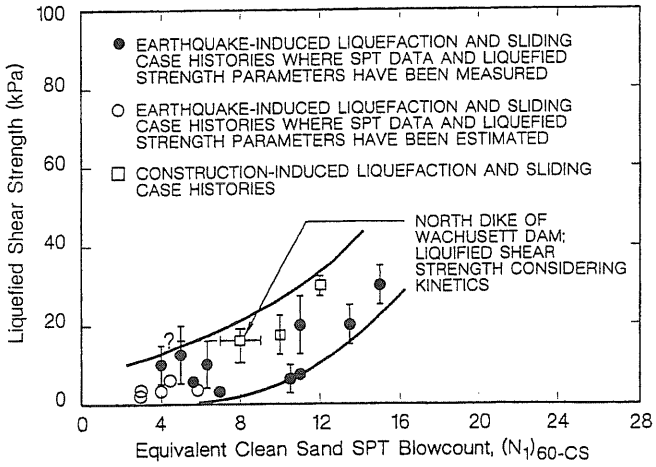

FIG. 9. Liquefied Shear Strength from North Dike of Wachusett Dam and Database Presented by Seed and Harder (1990)

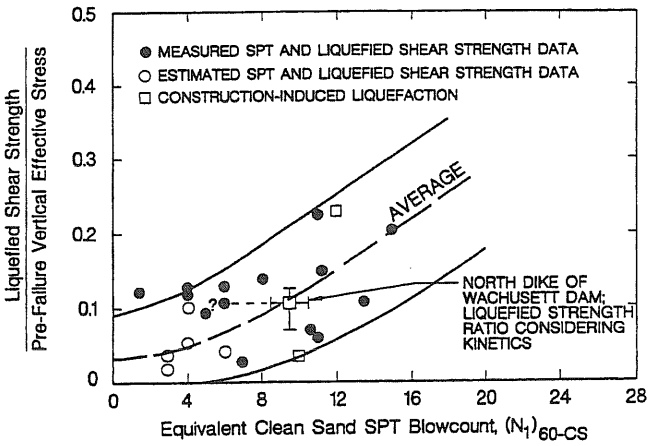

FIG. 10. Liquefied Shear Strength Ratio from North Dike of Wachusett Dam and Database Presented by Stark and Mesri (1992)

In summary, the values of liquefied shear strength and liquefied shear strength ratio back-calculated for the 1907 failure of the North Dike of Wachusett Dam agree with other case histories of liquefaction flow failure when the kinetics of failure are incorporated in the back-analysis. If kinetics are ignored, the shear strength back-calculated from the postfailure geometry can be extremely low (e.g., 3.8 kPa for the North Dike of Wachusett Dam) and unrepresentative of the shear strength mobilized during flow failure. Davis et al. (1988) and Castro (1995) reached a similar conclusion based on the analysis of three flow failure case histories. In addition, the back-

calculated shear strength from the prefailure geometry can be large (e.g., 37.6–41.9 kPa for the North Dike of Wachusett Dam). It appears that a liquefied shear strength of approximately 16.0 kPa and a liquefied shear strength ratio of approximately 0.106 (both of which include kinetics, potential hydroplaning, and nonliquefied soil shear strength effects) can be used for design purposes when stress, density, and soil conditions are similar to that of the North Dike of Wachusett Dam.

CONCLUSION

On April 11, 1907, during the first filling of Wachusett Dam reservoir, a static liquefaction flow failure occurred in the upstream slope of the eastern section of the North Dike of the dam. This fairly well-documented case history augments the limited number of flow failure case histories available in the literature. As concluded by Stark et al. (1998), understanding flow failure case histories is crucial to assigning a liquefied shear strength to soils susceptible to liquefaction. Case histories also provide the primary means to verify theoretical and laboratory assessments of the liquefied shear strength.

Four main conclusions can be drawn from this case history regarding the interpretation of other liquefaction case histories and the design or remediation of earth dams susceptible to liquefaction. First, the upstream fill soils consisted primarily of fine sands (median grain size, D_{50}, of approximately 0.42 mm and a fines content of 5–10%), were placed by uncontrolled dumping from carts, and received no compaction. As indicated by numerous investigators, moist fine sands, particularly when placed without compaction, tend to form a loose, collapsible structure. This appears to be the case at the North Dike of Wachusett Dam. Borings drilled in 1983 and 1991 that encountered upstream fill soils indicate that the fills had corrected SPT blowcounts, $(N_1)_{60}$, of approximately 7 bpf. When possible aging and postfailure consolidation under the remedial fill are considered, the upstream fill soils of the North Dike were probably very loose to loose, i.e., an $(N_1)_{60}$ of less than 7, and highly susceptible to liquefaction. In summary, sandy fills that subsequently will be saturated should not be placed without compaction, even in nonseismic regions, to resist static liquefaction.

Second, failure of the North Dike most likely occurred as a result of static liquefaction. Construction of the dike was complete and the reservoir was being filled at the time of the failure. No seismic or dynamic activity was reported in the vicinity of the failure. During failure, the upstream fill soils flowed approximately 100 m into the reservoir and dropped approximately 12.2 m in elevation. The failure mass came to rest below the reservoir water level at an angle of approximately 5 to 6 degrees, indicating that a low shear strength was available during the failure. The failure occurred over a former river channel where the dike reached a maximum height of 24.4 m and the driving shear stresses within the upstream fill were the largest. These observations and other evidence presented herein strongly suggest that liquefaction of the upstream fill soils occurred under the static driving shear stresses of the dike.

Third, this case history is unique because not only was the failure likely the result of static liquefaction, but loading probably was completely drained prior to liquefaction. Wachusett Reservoir was being filled for nearly three years prior to failure, and it is unlikely that any construction-induced or other excess porewater pressures existed in the upstream fill at the time of failure. Therefore, loading of the North Dike probably was fully drained. As the reservoir deepened, the vertical effective stress of the upstream sandy fill decreased significantly. However, about half of the dike was above the phreatic surface at the time of failure, and the driving shear stress had decreased by only about 15% due to reservoir filling. When the stress conditions reached the collapse surface (Sladen et al. 1985), the upstream fill liquefied and lost strength. Nearly identical drained stress paths have triggered liquefaction in laboratory tests (e.g., Sasitharan et al. 1993), however, to the authors' knowledge, this stress path has not previously been documented to trigger liquefaction in the field.

Fourth, the large difference between the shear strengths back-calculated form the prefailure and postfailure geometries suggest that kinetics, or momentum, played an important role in this liquefaction flow failure. In this case, a lower bound shear strength and strength ratio of approximately 3.8 kPa and 0.026, respectively, were back-calculated from the postfailure slope geometry. Using the prefailure slope geometry, an upper bound shear strength of 37.6–41.9 kPa and an upper bound shear strength ratio of 0.26–0.30 were back-calculated. Incorporating kinetics significantly affected the back-calculated shear strength. The kinetics analysis presented herein yielded a liquefied shear strength of approximately 16.0 kPa and a liquefied strength ratio of approximately 0.106. These values are roughly one-half the sum of the upper and lower bounds computed from the prefailure and postfailure geometries, respectively. These values of shear strength and shear strength ratio are considered "best estimates" for this case history and agree with other liquefaction case histories where kinetics were considered. Therefore, the liquefied shear strength and strength ratio obtained herein are recommended for design or remediation purposes for stress, density, and soil conditions similar to those in the North Dike of Wachusett Dam. In addition, the analysis methods presented herein can be used for design or remediation of other earth dams susceptible to liquefaction.

ACKNOWLEDGMENTS

The authors would like to thank the Metropolitan District Commission and the Massachusetts Water Resource Authority for permission to publish the details of this case history. The authors also would like to acknowledge the previous work conducted at this site by GZA GeoEnvironmental, Inc. of Upper Newton Falls, Mass., during the early 1990's. The current study was funded by the National Science Foundation, Grant Number 97-01785, as part of the Mid-America Earthquake Center (MAE Center) headquartered at the University of Illinois, Urbana-Champaign. The research was conducted as part of MAE Center Project GT-3, "Liquefaction Resistance of Soils." The second author also acknowledges the support provided by the William J. and Elaine F. Hall Scholar and University Scholar awards.

APPENDIX. REFERENCES

Baril, P. H., Wood, D. W., and Walton, W. H. (1992). "The Wachusett dam in the 21st century: modifications after 100 years of service." *Twelfth Annu. U.S. Comm. on Large Dams (USCOLD) Lecture Series*, Fort Worth, Tex., Vol. 1, 1–22.

Casagrande, A. (1965). "Second Terzaghi lecture: role of the 'calculated risk' in earthwork and foundation engineering." *J. Soil Mech. and Found. Div.*, ASCE, 91(4), 1–40.

Castro, G. (1995). "Empirical method in liquefaction evaluation." *Proc., 1st Annu. Leonardo Zeevaert Int. Conf.*, 1, 1–41.

Castro, G., Keller, T. O., and Boynton, S. S. (1989). "Re-evaluation of the lower San Fernando dam: report 1, an investigation of the February 9, 1971 slide." *U.S. Army Corps of Engrs. Contract Rep. GL-89-2*, Vols. 1 and 2, U.S. Army Corps of Engineers Waterways Experiment Station, Vicksburg, Miss.

Castro, G., Seed, R. B., Keller, T. O., and Seed, H. B. (1992). "Steady-state strength analysis of lower San Fernando dam slide." *J. Geotech. Engrg.*, ASCE, 118(3), 406–427.

Davis, A. P., Castro, G., and Poulos, S. J. (1988). "Strengths backfigured from liquefaction case histories." *Proc., 2nd Int. Conf. on Case Histories in Geotech. Engrg.*, St. Louis, Vol. IV, 1693–1701.

GZA GeoEnvironmental, Inc. (1991). "Wachusett Dam—Clinton, Massachusetts—north dike stability." *Stage I Report, Report to the Commonwealth of Massachusetts*, Vol. II, Metropolitan District Commission, Boston.

Haley & Aldrich, Inc. (1984a). "Report on phase II investigation, Wachusett reservoir dam, Clinton, Massachusetts." *Rep. Prepared for the*

Commonwealth of Massachusetts, Metropolitan District Commission, Boston.
Haley & Aldrich, Inc. (1984b). "Report on phase II investigation, Wachusett reservoir, north dike, south dike, Clinton, Massachusetts." *Rep. Prepared for the Commonwealth of Massachusetts*, Metropolitan District Commission, Boston.
Hazen, A. (1918). "A study of the slip in the Calaveras dam." *Engrg. News-Rec.*, 81(26), 1158–1164.
Liao, S. C., and Whitman, R. V. (1986). "Overburden correction factors for SPT in sand." *J. Geotech. Engrg.*, ASCE, 112(3), 373–377.
Mesri, G., Feng, T. W., and Benak, J. M. (1990). "Postdensification penetration resistance of clean sands." *J. Geotech. Engrg.*, ASCE, 116(7), 1095–1115.
Metropolitan District Commission. (1907). *Seventh annual report of the Metropolitan Water and Sewerage Board*, Commonwealth of Massachusetts, Boston.
Poulos, S. J., Castro, G., and France, J. W. (1985). "Liquefaction evaluation procedure." *J. Geotech. Engrg.*, ASCE, 111(6), 772–792.
Sasitharan, S., Robertson, P. K., Sego, D. C., and Morgenstern, N. R. (1993). "Collapse behavior of sand." *Can. Geotech. J.*, Ottawa, 30, 569–577.
Schmertmann, J. H. (1987). "Discussion of 'Time-dependent strength gain in freshly deposited or densified sand,' by J. K. Mitchell, and Z. V. Solymar." *J. Geotech. Engrg.*, ASCE, 113(2), 173–175.
Seed, H. B., Tokimatsu, K., Harder, L. F., and Chung, R. M. (1985). "Influence of SPT procedures in soil liquefaction resistance evaluations." *J. Geotech. Engrg.*, ASCE, 111(12), 1425–1445.
Seed, H. B. (1987). "Design problems in soil liquefaction." *J. Geotech. Engrg.*, ASCE, 113(8), 827–845.
Seed, R. B., and Harder, L. F. (1990). "SPT-based analysis of cyclic pore pressure generation and undrained residual strength." *Proc., H. B. Seed Memorial Symp.*, Bi-Tech Publishing Ltd., Richmond, British Columbia, Vol. 2, 351–376.
Skempton, A. W. (1985). "Residual strength of clays in landslides, folded strata and the laboratory." *Géotechnique*, London, 35(1), 3–18.
Sladen, J. A., D'Hollander, R. D., and Krahn, J. (1985). "The liquefaction of sands, a collapse surface approach." *Can. Geotech J.*, Ottawa, 22, 564–578.
Spencer, E. (1967). "A method of analysis of the stability of embankments assuming parallel interslice forces." *Géotechnique*, London, 17(1), 11–26.
Stark, T. D., and Eid, H. T. (1998). "Performance of three-dimensional slope stability methods in practice." *J. Geotech. and Geoenvir. Engrg.*, ASCE, 124(11), 1049–1060.
Stark, T. D., and Mesri, G. (1992). "Undrained shear strength of liquefied sands for stability analysis." *J. Geotech. Engrg.*, ASCE, 118(11), 1727–1747.
Stark, T. D., Olson, S. M., Kramer, S. L., and Youd, T. L. (1998). "Shear strength of liquefied soils." *Proc., Workshop on Post-Liquefaction Shear Strength of Granular Soils*, Univ. of Illinois at Urbana-Champaign, Urbana, Ill., ⟨http://mae.ce.uiuc.edu⟩.
Wright, S. G. (1990). *UTEXAS3—A computer program for slope stability calculations*, Shinoak Software, Austin, Tex.